JOURNAL OF CATALYSIS 51, 115–125 (1978)

Kinetic Data from a Pulse Microcatalytic Reactor–Hydrogenation of Benzene on a Nickel Catalyst

A. M. SICA, E. M. VALLES AND C. E. GIGOLA

Planta Piloto de Ing. Quimica, Universidad Nacional del Sur, Av. Alem 1253, Bahía Blanca, Argentina

Received December 31, 1976; revised August 29, 1977

The hydrogenation of benzene on a nickel catalyst has been studied by means of a pulse microcatalytic reactor in the 100–150°C temperature range. It is shown that the treatment of experimental data using equations derived for power-law and Langmuir–Hinshelwood rate models allows the determination of similar kinetic parameters as obtained from steady-state flow reactors.

INTRODUCTION

The pulse microcatalytic reactor has been extensively used in catalytic research, mainly as a qualitative tool to evaluate a series of catalysts. Some attempts have been made to use this technique for kinetic studies considering the simplicity of operation. However, the difficulties involved in the interpretation of experimental data have limited its application to the simple cases where the kinetics are linear and the reactant pulse moves along the reactor under ideal chromatographic conditions. In that case we can expect the conversion to be equal to that of flow reactors. Basset and Habgood (*1*) successfully applied the pulse technique to study the first-order isomerization of cyclopropane to propylene. Schwab and Watson (*2*) have provided another experimental example of the usefulness of the pulse technique by studying the dehydrogenation of methanol by the pulse and flow technique.

Analytical and numerical solutions of the related equations are, however, available for nonlinear kinetics (*3–5*), and they can be used to obtain quantitative information as long as the hypothesis of ideal chromatography is maintained. Bett and Hall (*6*) studied the dehydration of 2-butanol, a zero-order reaction, by pulse and steady-state flow methods. The results were not identical because the assumption of equilibrium adsorption was not valid. Blanton *et al.* (*4*) have successfully applied numerical solutions for gaussian input pulses to study the hydrogenation of ethylene on alumina. They found similar rate coefficients as derived from flow reactors. The hydrogenation of benzene and the dehydrogenation of cyclohexane were studied by Toyota and Echigoya (*7*) in a pulse reactor using a nickel on silica catalyst. Rate models previously found by the continuous flow technique were used together with the assumption of triangular input pulses to derive suitable equations for the analysis of kinetic data. For the former reaction, the assumption of a zero-order dependence on benzene concentration was inadequate, as the rate constant was found to be dependent on the amount of reactant in-

0021-9517/78/0511-0115$02.00/0

jected. Good kinetic results were obtained for the dehydrogenation reaction.

Recently (*8*), the kinetics of the oxidation of ethylene over a silver catalyst were studied by the pulse and flow technique. The experimental conditions were chosen to introduce a significant simplification of the continuity equation. The concentration of reactant in the gas phase was considered constant over the bed length and only dependent on time. The theoretical analysis leads to an equation which is only valid for small conversions. Despite the complexities of that system the rate constant for the formation of ethylene was similar to that obtained in the steady-state experiments.

Theoretical analysis of microreactors has received far more attention than experimental applications. Consequently, it was thought of interest to study the kinetics of a non-first-order reaction under pulsed conditions to test the validity of previous theory. We have confined our attention to the hydrogenation of benzene since it is a system for which extensive experimental data obtained from flow reactors are available for comparison. As mentioned above, a previous kinetic study in the pulse regime has met with limited success.

The reaction kinetics on nickel have been described by means of power-law rate equations with a first-order dependence on hydrogen pressure and zero or near-zero order with respect to benzene. The kinetics have also been correlated by a Langmuir–Hinshelwood type equation. A good review is given by Kehoe and Butt (*9*). At low temperature, 100–150°C, the reaction is irreversible, and the only product detected is cyclohexane. These features makes the reaction an appropriate one for kinetic studies in a microcatalytic reactor.

EXPERIMENTAL

Catalyst

The nickel on alumina was a commercial methanation catalyst available in the form of 6.35 by 6.35-mm pellets. It was ground to 30/40 sieve size and the nickel content as determined by the dimethylglyoxime method was 25%.

TABLE 1

Physical Properties of the Catalyst

Nickel content	25%
BET surface area	41 m^2/g
Apparent density	1.8 g/cm^3
Solid density	3.7 g/cm^3
Nickel surface area	7.4 $m^2/gcat$
Average pore radius	75 Å

Some physical data for the catalyst are listed in Table 1. The solid density and the apparent particle density were determined by the helium–mercury method. Using a conventional volumetric adsorption apparatus, hydrogen isotherms were measured at 250°C. The catalyst was previously reduced in flowing hydrogen at 400°C during 12 hr and evacuated at the same temperature for 6 hr. The net hydrogen uptake was obtained by extrapolation of the isotherm to zero pressure. In order to estimate the metal surface area, the value of 6×10^{-20} m^2 per hydrogen atom was used. The pore size distribution for this catalyst (obtained in an Aminco porosimeter) shows an average pore radii of 75 Å (1 Å = 10^{-10} m).

Apparatus

The equipment was similar to that described by Blanton *et al.* (*4*). Benzene pulses were introduced into a hydrogen carrier stream and passed through a dispersion column where sufficient pulse broadening was permitted in order to secure a slow concentration gradient along the catalyst bed. One flow-through thermal conductivity cell was placed before the reactor to measure the input pulse concentration. The fixed bed horizontal reactor was constructed of 4-mm-i.d. Pyrex glass tubing 0.36 m long and heated by an air bath. The catalyst particles were held in place by a fritted glass disk and a glass wool plug.

The remaining length of the reactor was filled with glass beads. The reaction temperature was measured with a thermocouple inserted in the center of the catalyst bed. After passing through the reactor, the hydrogen stream entered one side of a second thermal conductivity cell were the output pulse shape was measured. Chromatographic separation of reactant and product was then carried out using a 2.5-m column of Ucon Oil LB-550X on Chromosorb P 60/80, held at 110°C. The benzene and cyclohexane peaks were finally flowed through the other side of the same cell. The flow rate was measured at the outlet with a soap-film meter. The total pressure associated with every run was measured with a Wallace & Tiernan manometer. The pressure drop through the catalyst bed was negligible and it occurs mainly on the chromatographic column.

Procedure

Catalyst charges of 0.1 to 0.5 g were used, the amount being dependent on the temperature level. The catalyst was reduced in flowing hydrogen at 400°C during 12 hr and then cooled slowly to the reaction temperature. Experiments were carried out at five different temperatures between 100 and 150°C. Five to eight benzene pulses of different sizes were injected to obtain conversions in the 30–90% range at each temperature level. Between runs the catalyst was held under flowing hydrogen at the reduction temperature. The catalytic activity was constant, as no difference in conversion was noticed from pulses injected at different times under identical conditions. In order to determine the hydrogen pressure dependency on the rate of reaction, experiments were performed at 130°C at varying flow rates. In our experimental set up, it means changing the total pressure.

The method used to inject the benzene pulses deserves a special comment. They were introduced into the hydrogen stream using either a conventional gas saturator-sample valve device or via a chromatographic microsyringe. Despite its inherent limitations the method of microsyringe injection was preferred because of its simplicity. A standard 10-μl syringe was used in most runs. The former method has the advantage of more precise control of the amount injected, but it necessarily complicates the basically simple microreactor. Therefore it was only used for calibration purposes.

It was necessary to obtain triangular or gaussian pulses in order to treat the experimental data by means of previous derived equations. Gaussian pulses with a small tailing were obtained whatever the method of injection used. Analysis of input pulses traced on a high-speed recorder supported the assumption of triangular pulses. The concentration dependence on time is shown in Fig. 1.

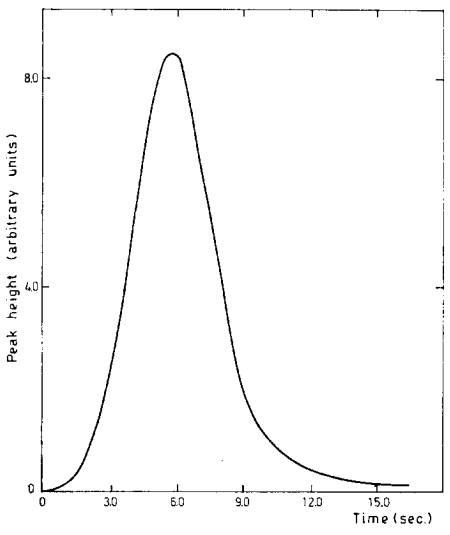

FIG. 1. Input pulse function.

Treatment of Data

As mentioned above, the kinetics of benzene hydrogenation on nickel catalysts have been described by power-law and Langmuir–Hinshelwood rate equations. When these rate models are introduced into the continuity equation for pulsed micro-

reactors, it is possible to obtain relatively simple mathematical expressions relating the conversion to the kinetic parameters (see Appendix). For a power-law rate equation,[1]

$$r = kp_{H_2}{}^m(c_B)^n = k'(c_B)^n, \qquad (1)$$

the relation is

$$X_B = 1 - \frac{\int_{T_1}^{T_2} \{[F(T-1)]^{1-n} + (n-1)K\}^{1/(1-n)}dT}{\int_0^{H/2} F(T)dT}, \qquad (2)$$

where $K = (kp_{H_2}{}^m c_0{}^{n-1})/Q = (k'c_0{}^{n-1})/Q$ under the restrictive assumption of ideal chromatography. In Eq. (2) the function to be integrated between T_1 and T_2 is the output pulse concentration. If triangular pulses are assumed

$$F(T) = 2T/H \quad \text{for} \quad T < H/2$$

and

$$T_1 = 1 + (H/2)(K(1-n))^{1/(1-n)},$$
$$T_2 = 1 + H/2.$$

When the rate equation is

$$r = (kk_a p_{H_2}{}^m c_B)/(1 + k_a c_B) = (k'k_a c_B)/(1 + k_a c_B), \qquad (3)$$

similar analysis leads to the following expression for the output pulse concentration:

$$C(T) = [F(T-1)] \times \exp\{K_a[F(T-1) - C(T)] - K\}, \qquad (4)$$

where

$$K = (kk_a p_{H_2}{}^m)/Q = k'k_a/Q, \quad K_a = k_a c_0.$$

[1] Nomenclature: c_B, benzene concentration; C, dimensionless concentration, c_B/c_0; $F(T)$, input pulse function; H, dimensionless pulse width; k, rate constant; k', pseudo rate constant; k_m, k_m', rate constants per unit mass of catalyst; k_a, adsorption coefficient; K_a, dimensionless adsorption coefficient; m, order of reaction with respect to hydrogen; n, order of reaction with respect to benzene; Q, flow rate; p_{H_2}, hydrogen partial pressure; r, rate of reaction per unit volume; r_m, rate of reaction per unit mass; T, dimensionless time; X_B, fractional conversion of benzene.

This equation can be solved by a trial and error procedure and then the total conversion can be evaluated as

$$X_B = 1 - \frac{\int_{T_1}^{T_2} C(T)dT}{\int_0^{H/2} F(T)dT}.$$

Plots of X_B vs K (n held constant) and X_B vs K_a (K held constant) are given elsewhere (*5*), together with a detailed derivation of Eqs. (2) and (4). Experimental data can be graphically fitted to the theoretical curves to obtain the kinetic parameters. For power-law kinetics the measured conversion is plotted versus the group $c_0{}^{n-1}/Q = K'$. Satisfactory fitting allows the determination of the reaction order n and the rate constant k', as K/K'. For Langmuir–Hinshelwood kinetics the conversion must be plotted versus c_0. In this case the fitting renders $k_a(K_a/c_0)$ and $k'k_a(K \times Q)$. The maximum input pulse concentration c_0 can be calculated from the recorder peak.

When Eqs. (2) and (4) are solved for $F(T)$ equal to $\exp(-T/H)^2$, the predicted results are identical to those for triangular pulses as long as n is smaller than one. For Langmuir–Hinshelwood kinetics the results are also similar. It appears therefore that the simplifying assumption of triangular pulses, although useful for the mathematical analysis, is not critical when considering practical application of microreactors.

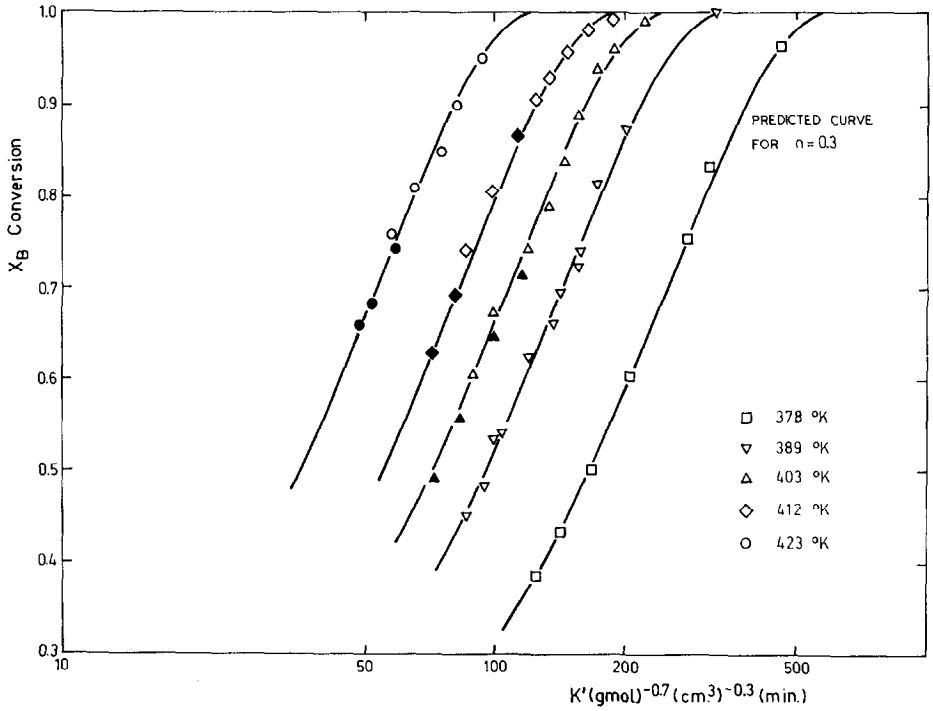

FIG. 2. Experimental data fitted by power-law kinetics. Variable temperature runs. Empty and full points on each curve indicate a different charge of catalyst. All K' values corrected for a mass of 0.378 g. Solid lines obtained by calculation.

RESULTS

Preliminary experiments were sufficient to suggest only a slight concentration dependence of the reaction rate on benzene concentration. It was observed that the cyclohexane peak area changed only a small amount regardless of the amount of benzene injected. The effect of benzene concentration and temperature on conversion, at constant flow rate, was first investigated and the results are shown in Fig. 2. The hydrogen pressure was assumed constant and equal to the total pressure, taking into account that the maximum benzene concentration for all runs was an order of magnitude smaller than the hydrogen concentration.

The same charge of catalyst was used for several runs, at each temperature, without observable deactivation. However, it was not possible to explore the whole temperature range using the same charge because it requires injection of too-small or too-large quantities of benzene. Therefore the amount of catalyst was sometimes selected in order to obtain adequate conversion at each temperature level.

In order to test the applicability of the power-law rate model (1) the results are compared with those predicted by Eq. (2). A reasonably good fit is observed for $n = 0.3$ at each temperature level. Values of the pseudo rate constant k' (which contains the hydrogen pressure term) were obtained from individual points on each curve. In Table 2 the calculation procedure is shown in detail for a typical run.

The effect of temperature is shown in Fig. 3 as an Arrhenius plot of the rate constant k_m' which was obtained as the mean value of those calculared at each temperature. The results from several runs are included, in addition to those of Fig. 2. These data yield an apparent activation energy of 10.1 ± 0.4 kcal/mol (1 kcal/mol = 4.19 kJ/mol).

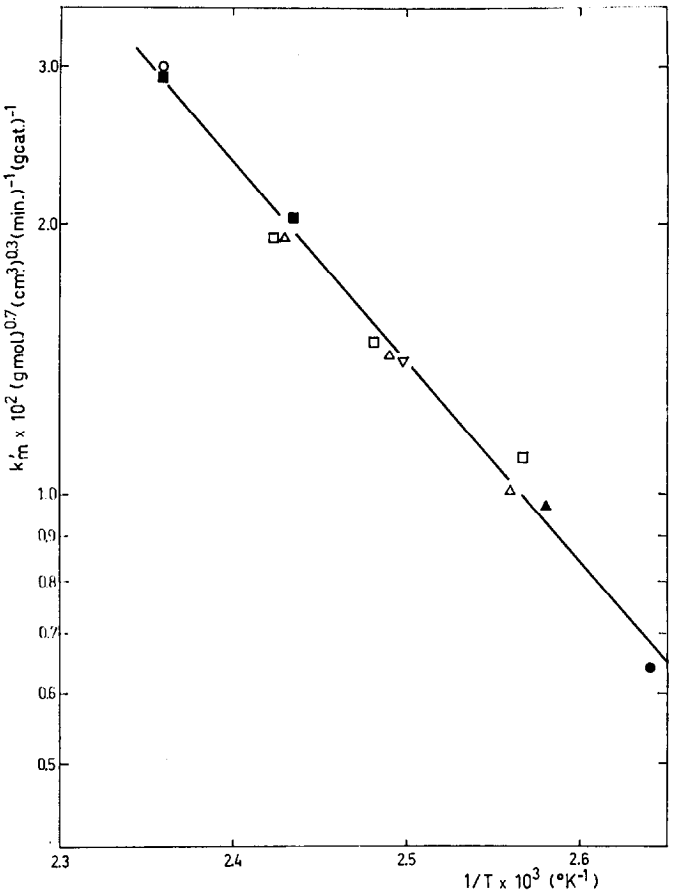

FIG. 3. Arrhenius plot for power-law kinetics. Each symbol corresponds to a different charge of catalyst.

As stated before, the total pressure was changed by modifying the flow rate. In this way the rate constant k' was calculated and plotted as a function of total pressure according to the relation $k' = k \cdot p_{H_2}{}^m$. As shown in Fig. 4, the order with respect to hydrogen is 1.25, for p_{H_2} varying between 950 and 1300 Torr (1 Torr = 133.3 N/m²).

Since orders with respect to individual reactants are known, the effect of concentration and flow rate can be correlated in a single curve. Figure 5 presents such a plot.

If the hydrogen pressure term is now removed from constant k_m', the true kinetics constant can be evaluated:

$$k_m = 0.80 \exp(-10.1/RT) \text{ (gmol)}^{0.7} \text{ (cm}^3\text{)}^{0.3} \text{ (min)}^{-1} \text{ (gcat)}^{-1} \text{ (Torr)}^{-1.25}.$$

TABLE 2
Summary of Data and Calculation Procedures for a Typical Run[a]

Conversion X_B	K'	K[from Eq. (2)]	$K/K' = k' \times 10^3$
1.000	323.6	1.36	4.20
0.874	201.5	0.84	4.17
0.743	158.3	0.66	4.17
0.661	136.5	0.568	4.16
0.698	143.3	0.60	4.18
0.815	173.5	0.72	4.15
0.624	119.6	0.50	4.18
0.534	98.7	0.418	4.19
0.483	94.4	0.39	4.13
0.450	85.6	0.357	4.17
0.541	140.6	0.437	4.17
0.722	150.6	0.63	4.18

[a] Mass = 0.378 g; T = 116.5°C; $k_m' = 1.1 \times 10^{-2}$ $\frac{\text{(gmol)}^{0.7}\text{ (cm}^3\text{)}^{0.3}}{\text{(min) (gcat)}}$.

As expected, the kinetic data were also consistent with a Langmuir–Hinshelwood rate model. To test Eq. (3), the conversion was plotted as a function of c_0, as shown in Fig. 6. From these data the influence of temperature on constants k_m and k_a was calculated leading to the Arrhenius plots of Fig. 7. They indicate an exothermic heat of chemisorption of 7.6 kcal/mol and an activation energy of 12.5 kcal/mol. The following equations can be written for the constants:

$$k_a = 90.4 \exp(7.6/RT) \text{ (cm}^3\text{)(gmol)}^{-1},$$

$$k_m = 0.397 \exp(-12.5/RT) \text{ (gmol) (min)}^{-1} \text{ (geat)}^{-1} \text{ (Torr)}^{-1.25}.$$

Under certain conditions, measured kinetics can reflect the effect of internal diffusion limitations. The absence of this type of restriction was estimated by the Weisz criterion and experimentally verified by a twofold reduction in particle size.

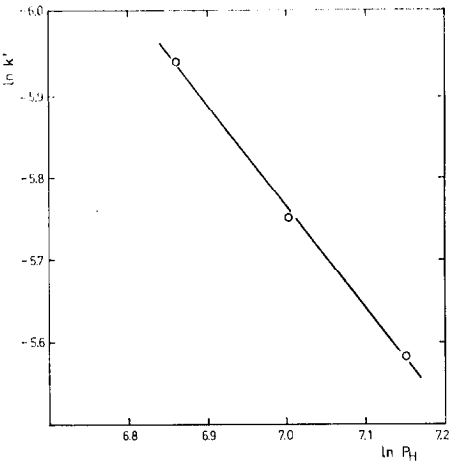

FIG. 4. Determination of hydrogen pressure dependence (T = 403°K). Each point is an average value of several data.

DISCUSSION

Two main conclusions can be drawn from these results. First, the equations derived for pulsed microreactors can be applied in a relatively simple way to study the ki-

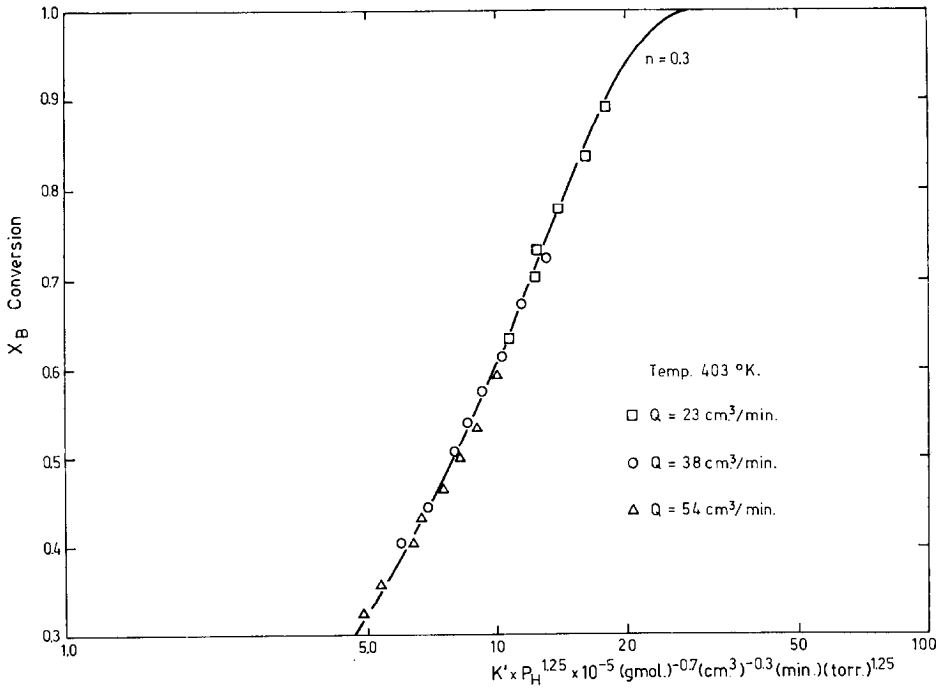

FIG. 5. Experimental data fitted by power-law kinetics. Variable flow rate runs.

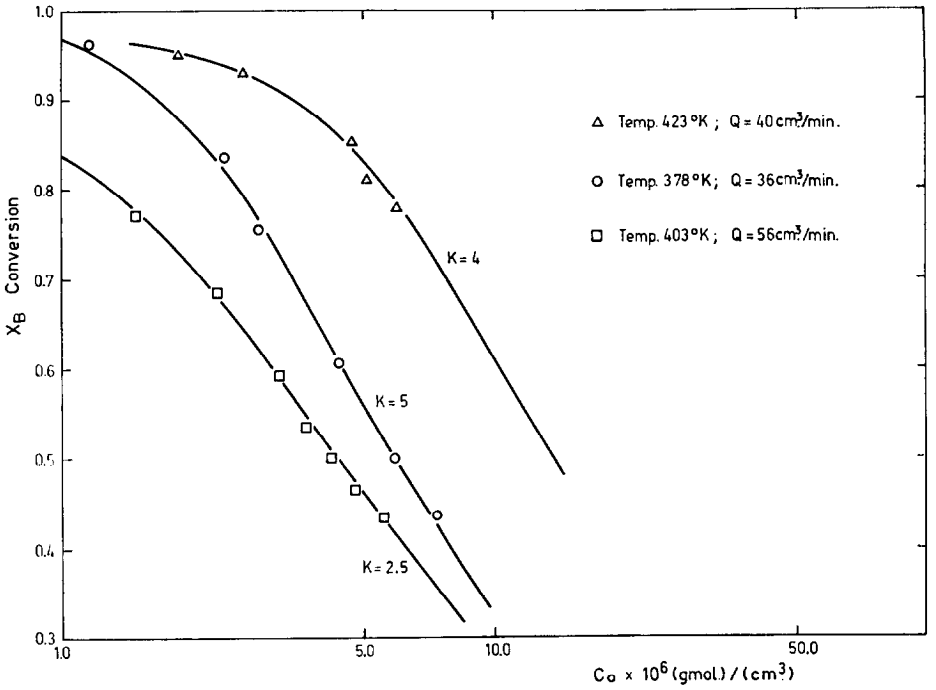

FIG. 6. Experimental data fitted by Langmuir–Hinshelwood kinetics. Variable temperature and flow rate runs.

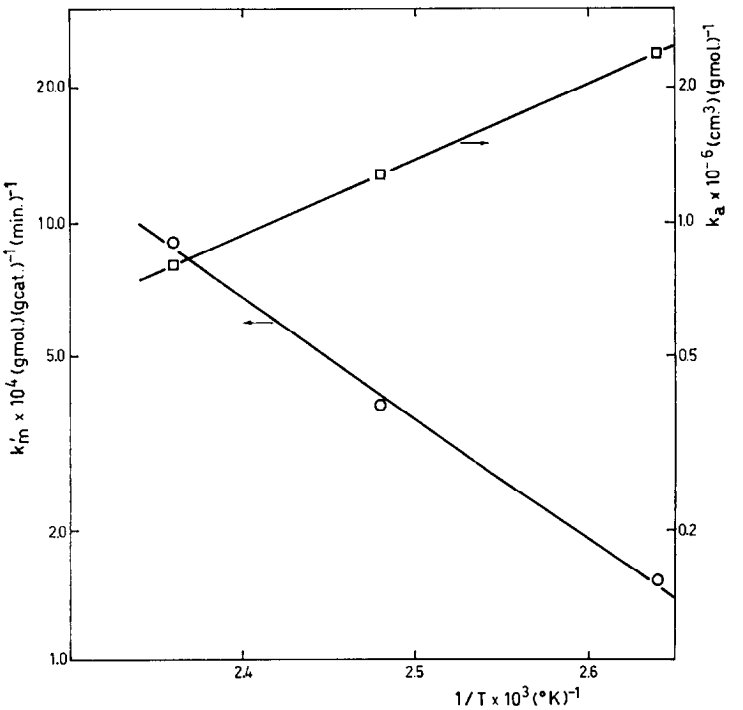

FIG. 7. Arrhenius plot for Langmuir–Hinshelwood kinetics.

netics of non-first-order reactions. Implicit in the use of those equations are a number of assumptions that were experimentally satisfied. For example, pulse broadening was not observed at the reactor end whatever the level of conversion, which proves the existence of equilibrium adsorption. Second, the main features of the kinetics are in agreement with those previously extracted from steady-state measurements: a fractional order with respect to benzene and near-first order with respect to hydrogen.

The following rate expression gives a good fit to the experimental data:

$$r_m = 0.80 \exp(-10.1/RT)(p_{H_2})^{1.25}(c_B)^{0.3}. \quad (5)$$

Taylor and Staffin (*10*) reported a 0.3 order with respect to benzene (for p_B varying between 9.88 and 68.4 Torr) and a 1.6 order with respect to hydrogen at 127°C, for a 5% Ni on silica catalyst. However, they found that both orders increased with increasing temperature, a behavior not observed in this work. An explanation for this discrepancy can be found in the narrow range of temperature explored and the higher benzene concentration (60.8–114 Torr) used in the present work. Under these conditions it seems possible to have a constant surface coverage and consequently a constant reaction order. In spite of the pronounced differences in the catalysts used, the specific activity is also comparable. They reported a value of 2×10^{-3} (gmol)/(hr)(m² Ni) at 127°C. Using the nickel surface area given in Table 1, the specific activity calculated at the same temperature and partial pressures is 0.6×10^{-3} (gmol)/(hr) (m² Ni). As the present experimental conditions were different, it is only possible to make the calculation if one assumes that the reaction orders are independent of pressure.

Another source of experimental data that can be used for comparison is the work of Germain *et al.* (*11*). They studied the hydrogenation of benzene on a coprecipitated nickel–alumina catalyst in the 120–190°C temperature range. At 140°C the benzene order was found to be 0.3, while the hydrogen order was near unity. The former value is coincident with our result. On the other hand, our value of 1.25 for hydrogen represents a reasonable approximation if one takes into account the assumptions involved.

The variations are larger when the apparent activation energies are compared. Our value of 10.1 kcal/mol does agree closely with the value of 11 kcal/mol found by Herbo (*12*) and Nicolai *et al.* (*13*) for supported nickel catalysts. However, Germain *et al.* found a value of 16 kcal/mol and Taylor and Staffin (*10*) reported an increase in activation energy from 6 to 10 kcal/mol depending on hydrogen partial pressure. The scatter in the results of the several studies is not surprising if one considers the variety of catalyst preparations and the differences in experimental conditions. The true activation energy may change with metal content or crystallite size. In addition, the surface coverage will be dependent on reactant partial pressure, which in turn may affect the heat of adsorption. As the influence of hydrogen partial pressure was only investigated at one temperature, it is not possible to draw any conclusion regarding its effect on the activation energy.

It was previously shown that the rate can also be described by a Langmuir–Hinshelwood equation,

$$r_m = \frac{0.397 \exp(-12.5/RT) \times 90.41 \exp(7.6/RT) c_B p_{H_2}^{1.25}}{1 + 90.41 \exp(7.6/RT) c_B}. \quad (6)$$

Although this study is not concerned with the reaction mechanism, the rate model is consistent with a Rideal–Eley scheme for the hydrogenation. A similar equation was used by Kehoe and Butt (*9*) to correlate kinetic data for a nickel on kieselguhr catalyst. They found m to be equal to 1, and the following values for the activation energy and the heat of adsorption: 12.29 and −8.26 kcal/mol, respectively. The agreement with our values is remarkable.

As it is often the case, different rate models such as Eqs. (5) and (6) give a satisfactory correlation of the kinetic data. This result is not unexpected if one observes that Eqs. (2) and (4) predict similar conversion versus c_0 curves for both models. An experimental way to distinguish between the two possibilities has been proposed (*5*), based on the pulse-narrowing effect due to chemical reaction. However, for practical applications the method requires the specific detection of the reactant pulse at the reactor exit, an objective which is difficult to accomplish experimentally.

Therefore the information available does not permit us to choose between the two alternatives, a situation which is normally the case for continuous flow experiments.

The good agreement of the kinetic parameters obtained in this investigation with those of more conventional techniques substains the belief that pulse reactors are suitable for kinetic studies. Although the results presented here are not novel, and the application to other catalytic reactions cannot be guaranteed, they are important considering the extensive use of the hydrogenation of benzene as a test reaction in catalysis.

APPENDIX: DERIVATION OF EQUATIONS (2) AND (4)

The mass balance for a pulse of reactant passing through an isothermal and isobaric bed of length L is given by the following system of partial differential equations:

$$\partial c_B/\partial t + \partial q_B/\partial t + u_c(\partial c_B/\partial y) - D_{ef}(\partial c_B{}^2/\partial y^2) + k_1(q_B)^n = 0, \quad (1a)$$

$$\partial q_B/\partial t = k_2 c_B - k_1 q^n - k_3 q_B, \quad (2a)$$

where u_c is the carrier gas velocity, D_{ef} is the effective diffusivity, q_B is the surface concentration of reactant, and k_1, k_2, and k_3 are the surface reaction rate constant, the adsorption rate constant, and the desorption rate constant, respectively. It is assumed that the chemical reaction at the surface of the catalyst can be described by a power-law rate equation. If the assumptions of ideal chromatography are valid the system can be reduced to a single equation:

$$\partial c_B/\partial t + u(\partial c_B/\partial y) + (k_1 a^n c_B{}^n)/(1 + a) = 0. \quad (3a)$$

The pulse velocity u is:

$$u = u_c/[1 + (k_2/k_3)] = u_c(1 + a).$$

Dimensionless variables can be defined as follows: $T = tu/L$, $C = c_B/c_0$, $Y = y/L$, where c_0 is the maximum concentration of the input pulse. Equation (3a) transforms to

$$\partial C/\partial T + \partial C/\partial Y + KC^n = 0, \quad (4a)$$

where K is the Damköhler number defined as

$$K = (k_1 a^n c_0{}^{n-1} L)/u_c.$$

If the carrier gas flow rate Q is used instead of the gas velocity, the dimensionless number can be written

$$K = (k_1 a^n c_0{}^{n-1} V)/Q = (k' c_0{}^{n-1})/Q,$$

where V is the reactor void volume.

The proper boundary conditions for Eq. (4a) are: $C(Y, Y) = 0$, $C(0, T) = F(T)$ for $T > 0$, where $F(T)$ describes the input pulse concentration.

In order to solve Eq. (4a) a new set of variables is defined: $Y' = Y$, $T' = T - Y$, where T' is the time passed since the first molecules arrived at point Y. Equation

(4a) now transforms to

$$\partial C'/\partial Y' + KC'^{n} = 0. \qquad (5a)$$

For all $n \neq 1$, the solution is

$$C(Y, T)^{1-n} = \{[F(T - Y)]^{1-n} + (n - 1)KY\}^{+}. \qquad (6a)$$

The right-hand side of Eq. (6a), being negative for $T = Y$ and $n < 1$, does not satisfy the boundary condition $C(Y, Y) = 0$. The apparent inconsistency can be explained on grounds that, for reaction order less than unity, the pulse width is reduced by chemical reaction; so, the time needed for the pulse to reach a given point will be larger than the value predicted from the pulse velocity. To solve this problem, a restriction must be imposed on the right-hand side of Eq. (6a), that is, to consider only its positive values.

Now the total conversion at the reactor exit can be calculated as

$$X = 1 - \frac{\int_{T_1}^{T_2} C(1, T)dT}{\int_{0}^{H/2} C(0, T)dT}, \qquad (7a)$$

where H is the pulse width in dimensionless form. Combination of Eqs. (6a) and (7a) gives Eq. (2).

The limit T_2 is equal to the residence time of the pulse maxima. The limit T_1 is obtained from Eq. (6a) setting Y equal to one and C equal to zero.

By means of the same simplifying assumptions, an equation similar to (4a) can be obtained for a Langmuir–Hinshelwood rate model:

$$\partial C/\partial T + \partial C/\partial Y + KC/(1 + K_aC) = 0.$$

The solution to this equation obtained by the same procedure used before gives Eq. (4).

ACKNOWLEDGMENT

The authors are grateful to Prof. J. Hightower for his continued support of this work.

REFERENCES

1. Basset, D. W., and Habgood, H. W., *J. Phys. Chem.* **64**, 769 (1960).
2. Schwab, G. M., and Watson, A. M., *J. Catal.* **4**, 570 (1965).
3. Gaziev, G. A., Filinovskii, V. Y., and Yanovskii, M. I., *Kinet. Katal.* **4**, 688 (1963).
4. Blanton, W. A., Byers, C. H., and Merrill, R. P., *Ind. Eng. Chem. Fundam.* **7**, 611 (1968).
5. Sica, A. M., Valles, E. M., and Gigola, C. E., *Lat. Amer. J. Chem. Eng.* **4**, 109 (1974).
6. Bett, J. A. S., and Hall, W. K., *J. Catal.* **10**, 105 (1968).
7. Toyota, K., and Echigoya, E., *Kagaku Kogaku* **32**, 1005 (1968).
8. Verma, A., and Kagliaguine, S., *J. Catal.* **30**, 430 (1973).
9. Kehoe, J. P., and Butt, J. B., *J. Appl. Chem. Biotechnol.* **22**, 23 (1972).
10. Taylor, W. F., and Staffin, H. K., *J. Phys. Chem.* **71**, 3314 (1967).
11. Germain, J. E.. Maurel, R., Bourgeois, Y., and Sinn, R., *J. Chim. Phys.* **60**, 1219 (1963).
12. Herbo, C., *J. Chim. Phys.* **47**, 454 (1950).
13. Nicolai, J., Martin, R., and Jungers, J. C., *Bull. Chim. Belg.* **57**, 555 (1948).